

## Article

# Development of Transethosomes Loaded with Fruit Extract from *Carissa carandas* L. as a Brightening and Anti-Aging Cosmeceutical Ingredient

Sitthiphong Soradech \*, Worawan Tiatragoon, Phongsapak Phanphothong, Kanyarat Ouamkan, Pattarawadee Kengkwasingh, Supatjaree Ruengsomwong, Somkamol Intawong and Thanchanok Muangman

Expert Centre of Innovative Herbal Products, Thailand Institute of Scientific and Technological Research, Khlong Luang, Pathum Thani 12120, Thailand; worawan@tistr.or.th (W.T.); phanphothong.ph@gmail.com (P.P.); kanyarat.ok08@gmail.com (K.O.); pattarawadee@tistr.or.th (P.K.); supatjaree@tistr.or.th (S.R.); somkamol@tistr.or.th (S.I.); thanchanok@tistr.or.th (T.M.)

\* Correspondence: sitthiphong@tistr.or.th; Tel.: +66-(0)-2577-9013

**Abstract:** The ethanolic extract of *Carissa carandas* L. (ECE) inhibited the enzyme tyrosinase, enhanced the proliferation of normal human dermal fibroblast cells, and increased the formation of collagen type I, indicating possible anti-aging and whitening effects. However, the stratum corneum acts as a rate-limiting stage in the absorption of herbal extracts through the skin, resulting in limited absorption of ECE via the skin, which affects the efficacy of ECE. The purpose of this study was to develop ECE encapsulated in transethosomes for improved skin penetration as a novel brightening and anti-aging cosmeceutical ingredient. Transethosomes were successfully developed using the sonication technique, with a suitable formulation including 1.00% (*w/w*) phosphatidylcholine, 0.10% (*w/w*) polysorbate 80 and 28.55% (*v/v*) ethanol. The physicochemical properties, encapsulation efficacy, in vitro skin permeation and toxicity of ECE-loaded transethosomes were also investigated. The result showed that the percentages of encapsulation of ECE loaded in transethosomes increased slightly with higher concentrations of the ECE. When compared to the liquid extract, the ECE loaded in transethosomes significantly increased ( $p < 0.05$ ) skin penetration. Furthermore, ECE loaded with transethosomes showed low cytotoxicity in normal human dermal fibroblast cells and caused no skin irritation when evaluated on reconstructed human epidermal skin. Given these abilities, it is evident that transethosomes containing ECE are highly effective anti-aging and skin-whitening agents, making them a promising new cosmeceutical ingredient.

**Keywords:** *Carissa carandas* L.; transethosomes; anti-aging; brightening; cosmeceutical ingredient



**Citation:** Soradech, S.; Tiatragoon, W.; Phanphothong, P.; Ouamkan, K.; Kengkwasingh, P.; Ruengsomwong, S.; Intawong, S.; Muangman, T. Development of Transethosomes Loaded with Fruit Extract from *Carissa carandas* L. as a Brightening and Anti-Aging Cosmeceutical Ingredient. *Cosmetics* **2024**, *11*, 199. <https://doi.org/10.3390/cosmetics11060199>

Academic Editors: Bruno Fonseca-Santos and Marlus Chorilli

Received: 21 September 2024  
Revised: 13 November 2024  
Accepted: 18 November 2024  
Published: 21 November 2024



**Copyright:** © 2024 by the authors. Licensee MDPI, Basel, Switzerland. This article is an open access article distributed under the terms and conditions of the Creative Commons Attribution (CC BY) license (<https://creativecommons.org/licenses/by/4.0/>).

## 1. Introduction

*Carissa carandas* L. (*Apocynaceae*), often known as Karanda, is widely used as a medicinal herb. It is a large dichotomously branched evergreen shrub with short stems and strong thorns in pairs. It is also effective for anti-oxidant, anti-tyrosinase, anti-microbial, wound healing, fever reduction, and heart disease [1–4]. This fruit extract has found the phytochemical constituents, including Vitamin C, anthocyanin, flavonoids, glycosides, alkaloids, carbohydrates, sterols, terpenoids, tannins, and saponins [2,3]. The extract contains potent antioxidants, such as bioflavonoids and anthocyanins, which can help delay aging and reduce wrinkles. A study found that *C. carandas* L. extract effectively inhibited the growth of *Pseudomonas aeruginosa*, *Staphylococcus aureus*, and *Escherichia coli* more effectively than gentamicin [5]. In addition, the extract has wound-healing and anti-inflammatory properties, particularly in chronic wounds [4,6] and exhibits anti-bacterial activity [3]. Additionally, ethanolic *C. carandas* L. extract has been found to inhibit the enzymes MMP-2 and MMP-9, which are responsible for collagen degradation, as well as hyaluronidase, an enzyme associated with the breakdown of hyaluronan in the skin [7]. These findings indicate

that *C. carandas* L. extract has the potential to be used as an active ingredient in brightening and anti-aging cosmeceutical products.

Currently, there have been progress in the development of different techniques to deliver active ingredients derived from herbal extracts, with the aim of increasing the efficacy of these compounds and enhancing their absorption through the skin. Physical techniques include iontophoresis, sonophoresis, microneedles, and drug delivery systems such as liposomes, niosomes, and micelles [8]. The stratum corneum acts as a rate-limiting stage in the absorption of active compounds from plants or herbs through the skin. The outermost layer of the epidermis, known as the stratum corneum, provides the purpose of protecting the skin against contamination, toxic substances, and other outside elements. The protective structure of this design leads to limited absorption of drugs via the skin, which affects the efficacy of drug or active ingredients [8,9]. However, these issues can be addressed using drug delivery systems such as transethosomes, which are highly flexible vesicles developed from ethosomes and transferosomes. They consist of phospholipids, ethanol, and edge activators from non-ionic surfactants, which can encapsulate both hydrophilic and lipophilic substances. Transethosomes can penetrate the skin in a flexible, deformable vesicular form, adapting their shape as they move through the skin. The advantages of transethosomes include their ability to penetrate deeply into the skin, protect active substances from degradation due to moisture, extend shelf life, and shield substances from sunlight and oxidation. They also enhance the penetration of active compounds and deliver them to targeted sites, exhibiting the ability to squeeze through gaps between cells, due to their flexible nature and the ethanol component, which improves lipid membrane fluidity [10,11]. Previous studies have shown that transethosomes improve the penetration of active substances, enhance their effectiveness on target cells, and increase anti-oxidant activity [12,13]. Given these properties, it is evident that *C. carandas* L. extract has the potential for development into a cosmeceutical active ingredient for anti-aging and skin brightening. By enhancing its efficacy and stability through encapsulation in transethosomes, it could improve effectiveness, cellular delivery, biocompatibility, and skin penetration, while also adding market value to the cosmetic industry.

As previously stated, the development of a cosmeceutical ingredient based on *C. carandas* L. was an important research topic to study. Hence, the goal of this research was to extract *C. carandas* L. (ECE) and to explore its biological and toxicological activities as anti-aging and brightening effects. It was then used to develop and evaluate transethosomes, which could be employed as a new cosmeceutical agent for rejuvenation and skin whitening.

## 2. Materials and Methods

### 2.1. Materials

Phosphatidycholine (80%, purified) was purchased from Myskinrecipes (Bangkok, Thailand), Polysorbate 80 was purchased from Chem Supply Pty Ltd. (Gillman, SA, Australia), absolute ethanol was purchased from RCI Labscan (Bangkok, Thailand), Roswell Park Memorial Institute media (RPMI 1640) and anti-biotic-anti-mycotic (streptomycin) were purchased from PAA Laboratories GmbH (Cölbe, Germany), Fetal bovine serum (FBS) was purchased from Gibco (Grand Island, NY, USA) resazurin (Sigma Aldrich, St. Louis, MO, USA), and *Carissa carandas* fruit was purchased from Amphawa, Samut Songkhram Province, Thailand.

### 2.2. Extraction of *C. carandas* L.

Briefly, 200 g of dried *C. carandas* L. fruit was extracted with a mixture of ethanol and water using ultrasonication technique at room temperature ( $27 \pm 2$  °C) for 30 min. The extract was filtered through the paper filter Whatman No. 1, connected with a vacuum pump. The residues were re-extracted more by the same process twice. All filtrates were collected, pooled and dried by a rotary evaporator (Rotavapor R210, Buchi, Switzerland)

at 40 °C. The crude extracts were kept at −80 °C until use. The percentage yield was calculated as Equation (1).

$$\% \text{ Yield} = (\text{The weight of plant extract} / \text{weight of the dried plant sample used}) \times 100 \quad (1)$$

### 2.3. Determination of Malic Acid in ECE

Furthermore, 70 mg of ECE were precisely weighed and extracted with 70% ethanol. The extract was then extracted again with 0.01 M  $\text{KH}_2\text{PO}_4$  (pH 2.3 buffer) in a 25 mL container for 10 min using an ultrasonic bath. After the solution had cleared, the volume was adjusted to 50 mL in a volumetric flask containing 0.01 M  $\text{KH}_2\text{PO}_4$  (pH 2.3 buffer). The resulting solution was filtered through a 0.2  $\mu\text{m}$  syringe filter before being analyzed using HPLC. The malic acid content of ECE was then determined using a Waters Alliance 2695 LC system (Milford, MA, USA) connected to a Waters model 2996 photodiode array detector (PDA). Data collection and processing were carried out using an Empower workstation. The optimum HPLC system used a  $\text{C}_{18}$  reverse phase column (Phenomenex Luna C18, 150  $\times$  4.6 mm i.d., particle size 5  $\mu\text{m}$ , Torrance, CA, USA). The isocratic was eluted using phosphate buffer pH 2.3 at a flow rate of 0.5 mL/min, and PDA was detected at 210 nm. The temperature of the column was kept at  $25 \pm 5$  °C. The injection volume was 20  $\mu\text{L}$ . The overall run time was 30 min per sample.

### 2.4. Determination of Cytotoxicity and Biological Activities of ECE

#### 2.4.1. Cytotoxicity Test in Melanoma Cell ( $\text{B}_{16}\text{F}_{10}$ )

$\text{B}_{16}\text{F}_{10}$  melanoma cells (ATTC CRL-6475<sup>TM</sup>, Manassas, VA, USA) were grown as a monolayer in Roswell Park Memorial Institute media (RPMI 1640; PAA, Pasching, Austria), supplemented with 10% heat-inactivated fetal bovine serum (FBS; Gibco, PA, USA), 100 units/mL penicillin, and 0.1 mg/mL streptomycin (anti-biotic-anti-mycotic; PAA, Pasching, Austria). The cultures were housed in a humidified atmosphere with 5%  $\text{CO}_2$  at 37 °C, with the medium being replaced every 2 days. The conversion of resazurin (Sigma, MO, USA) to resorufin, a cellular health indicator, happens in the cytoplasm of living cells. Resazurin, a non-toxic blue and practically non-fluorescent compound, changes in live cells to red, highly fluorescent resorufin, causing enhanced fluorescence and an apparent color change in the surrounding media.  $\text{B}_{16}\text{F}_{10}$  murine melanoma cells were planted in 96-well plates with a density of  $10^4$  cells per well. After 48 h of incubation with 50  $\mu\text{g}/\text{mL}$  extracts, 20  $\mu\text{L}$  of resazurin (14 mg/dL) was added to each well, and absorbance was measured at 570 and 600 nm after 4 h of incubation at 37 °C. Cells treated with 0.05% dimethyl sulfoxide (DMSO) and kojic acid served as vehicle and positive controls, respectively, with background measurements taken from the culture media. All experiments were conducted in triplicate.

#### 2.4.2. Cytotoxicity in Normal Human Dermal Fibroblast Cells

Primary Dermal Fibroblast Cells (Normal, Human, Adult; HDFa; ATTC PCS-201-012<sup>TM</sup>, Manassas, VA, USA) were seeded into a 96-well plate at a density of  $1 \times 10^5$  cells/mL and incubated for 24 h. Various concentrations of test samples, dissolved in DMSO (200  $\mu\text{L}$ , ranging from 10 to 1000  $\mu\text{g}/\text{mL}$ ), were added to the cells and incubated for an additional 24 h. After incubation, the samples were removed, and the cells were washed. Following washing, 50  $\mu\text{L}$  of MTT (3-(4, 5-dimethylthiazolyl)-2, 5-diphenyltetrazolium bromide) solution (5 mg/mL) and 150  $\mu\text{L}$  of medium were added to each well. The plate was then incubated at 37 °C with 5%  $\text{CO}_2$  for 4 h. The medium containing MTT was discarded, and the resulting MTT formazan was dissolved by adding 150  $\mu\text{L}$  of DMSO with gentle agitation for 15 min. The absorbance was measured at 540 nm. The extract's cytotoxicity was assessed by determining the  $\text{IC}_{50}$ , defined as the concentration that inhibits 50% of cell viability.

#### 2.4.3. Determination of Tyrosinase Inhibition

The extracts were tested using the modified tyrosinase inhibition method previously published [14]. In a 96-well plate, 120  $\mu\text{L}$  of 1.66 mM tyrosine solution prepared in 0.1 M phosphate buffer (pH 6.8), 60  $\mu\text{L}$  of five serial concentrations of plant extracts (ranging from 0.001 to 10 mg/mL, diluted in a 1:1 mixture of methanol and 20% *v/v* DMSO), and 60  $\mu\text{L}$  of phosphate buffer were combined. The mixture was incubated at  $37 \pm 2$  °C for 1 h. Following incubation, 60  $\mu\text{L}$  of tyrosinase enzyme solution (0.6 mg/mL in phosphate buffer) was added to each well. Enzyme activity was then measured using a microplate reader set to 450 nm. For comparison, alpha-arbutin and kojic acid (both at 0.1 mg/mL) were used as positive controls. The  $\text{IC}_{50}$  value, defined as the concentration of the extract required to inhibit 50% of tyrosinase activity, was determined. Tyrosinase inhibition (%) was calculated according to Equation (2).

$$\% \text{ Tyrosinase inhibition} = \frac{(\text{Abs control} - \text{Abs sample})}{(\text{Abs control})} \times 100 \quad (2)$$

#### 2.4.4. Determination of Cellular Tyrosinase Activity

Tyrosinase activity was assessed using a spectrophotometric method by tracking the oxidation of DOPA to dopachrome. B<sub>16</sub>F<sub>10</sub> melanoma cells ( $5 \times 10^4$  cells/well) were seeded into a 96-well plate, incubated for 24 h, and treated with a 50  $\mu\text{g}/\text{mL}$  extract. Following trypsinization, the cells were collected, pelleted, and washed with PBS. The cell pellets were lysed in 100  $\mu\text{L}$  of 100 mM sodium phosphate buffer (pH 6.8) containing 1% Triton X-100 and 0.1 mM PMSF. After 30 min, the lysates were centrifuged at 10,000 rpm for 20 min at 4 °C. The resulting supernatant was transferred to a sterile 1 mL microtube and stored at  $-80$  °C. In a 96-well plate, 100  $\mu\text{L}$  of the protein suspension was combined with 100  $\mu\text{L}$  of 5 mM DOPA. After a 2 h incubation, absorbance was recorded at 475 nm.

#### 2.4.5. Determination of Cell Proliferation Activity

The ECE was tested for cell proliferation activity in normal human dermal fibroblasts using the SRB assay described by Manosroi et al. [15]. Ascorbic acid (50  $\mu\text{g}/\text{mL}$ ) was utilized as a positive control. The cells were plated at a density of  $1 \times 10^5$  cells/well in 96-well plates and allowed to attach overnight in 5%  $\text{CO}_2$  at 37 °C. Cells were subsequently treated to the extracts at both doses (0.5 and 1 mg/mL) for 24 h. Following incubation, the adhering cells were fixed in place, washed, and stained with SRB. The bound dye was solubilized, and absorbance was measured at 540 nm using a well reader. The assays were carried out in three different and separate experiments. The proportion of cell proliferation was calculated using Equation (3).

$$\% \text{ Cell proliferation} = \frac{(A \text{ sample} - A \text{ blank})}{(A \text{ control} - A \text{ blank})} \times 100 \quad (3)$$

#### 2.4.6. Determination of Stimulate Collagen Production

Normal human dermal fibroblast cells (ATCC CRL-1474, Manassas, VA, USA) were grown in Dulbecco's Modified Eagle's Medium (DMEM) supplemented with 10% fetal bovine serum, 2 mM L-glutamine, and 100 unit/mL penicillin and streptomycin. The cells were incubated in a humidified 5%  $\text{CO}_2$  atmosphere at 37 °C for 72 h. The cells were seeded in a 6-well plate at a density of  $2 \times 10^5$  cells/mL and incubated for 24 h. After that, the media were removed and added with different concentrations of extract (50, 100, and 200  $\mu\text{g}/\text{mL}$ ), incubated continually for 24 h and the extracts were then removed. The supernatant was detected for collagen using COL1A1 AlphaLISA assay kits (Perkin Elmer Inc., Shelton, CT, USA) according to the manufacturer's instructions. After that, the percentage of collagen stimulation was generated with the following Equation (4).

$$\% \text{ Collagen stimulation} = \frac{(AC - AT)}{AC} \times 100 \quad (4)$$

AC = the collagen concentration of the control

AT = the collagen concentration of the test sample

### 2.5. *In Vitro* Skin Irritation Testing

Both samples, ECE and ECE loaded in transethosomes, were tested for in vitro skin irritation using the standard method OECD test guideline No439: Reconstructed Human Epidermis Test Methods. Briefly, the SkinEthic™ RHE/reconstructed human epidermis tissues were treated with the sample for 42 min at room temperature. PBS and 5% SDS were employed as the negative and positive controls, respectively. All tissues were washed with PBS and incubated for 42 h at 37 °C and 5% CO<sub>2</sub>. Cell viability (%) was determined using the MTT conversion assay. In vitro interpretation criteria include non-irritant tissue replicates with a mean viability of more than 50% and irritant tissue replicates with a mean viability of less than 50%.

### 2.6. *Transethosomes* Preparation

Phosphatidylcholine and edge activators (polysorbate 80, PEG-40 hydrogenated castor oil, or polysorbate 20) were dissolved in ethanol and subsequently agitated using a magnetic stirrer at 600 RPM until a uniform solution was formed (Part I). After that, the extract of ECE was dissolved in ethanol. Subsequently, 500 µL of propylene glycol was added and stirred with a magnetic stirrer at 600 rpm until a transparent pink solution was achieved (Part II). Next was incorporating the mixture of Part I into the mixture of Part II. The formulation added preservative and adjusted an appropriate volume to 100 mL using deionized water. The mixture was agitated constantly using a magnetic stirrer set at 600 RPM for 15 to 30 min. Subsequently, transethosomes were generated, including several methods, as outlined in Table S1.

### 2.7. *Effect of Concentrations of ECE Loaded in Transethosomes*

The sonication technique was employed to prepare transethosomes with different concentrations of ECE (Table S2). In a 100-mL vial, 1.0 g phosphatidylcholine and 0.1 g Tween 80 were dissolved in 13.55 mL of 70% ethanol using a stirrer set at 600 rpm (Part I). In 15 mL of 70% (*v/v*) ethanol, ECE at concentrations of 0.5% (0.5 g), 1.0% (1.0 g), and 2.0% (2.0 g) (*w/v*) was dissolved. Subsequently, 500 µL of propylene glycol was added (Part II). The mixture in Part I was combined with the mixture in Part II at the interface. A preservative was added to the formulation, and the volume was adjusted to 100 mL using deionized water. The mixture was then stirred continuously at a speed of 700 rpm. The suspension was prepared to form transethosomes using an ultrasonic probe (Hielscher UP400St, Teltow, Germany) at 40 amplitudes and a pulse rate of 10% for 5 min. The total transethosomes volume was 100 mL.

### 2.8. *Size, Polydisperse Index (PDI), and Zeta Potential Measurement*

Size, polydispersity index (PDI), and zeta potential were measured using dynamic light scattering (DLS) and electrophoretic light scattering (ELS) with the Zeta sizer Nano ZS (Malvern Panalytical Ltd. in Malvern, UK). Prior to testing, the samples were 100-fold diluted with deionized water.

### 2.9. *Morphology*

The morphology of nanoparticles was observed under a Transmission Electron Microscope (TEM) model Hitachi HT7700 (Tokyo, Japan) at 80 kV. The blank transethosomes and ECE loaded in transethosomes were prepared by diluting 20 and 50-fold with DI water, respectively. Both were dropped onto a carbon-copper grid, waited for 30 min, and subsequently stained with 1% uranyl acetate.

### 2.10. Determination of Entrapment Efficiency (%EE) and Drug Loading Capacity (%LC)

The Amicon centrifugal filter tube (30 kDa, Merk Millipore in Cork, Ireland) was used to evaluate the encapsulation efficiency (%EE). A volume of 1 mL of transethosomes was added to the tube and subjected to centrifugation at 5000 g (RCF) for 30 min. The obtained precipitate and supernatant were diluted in methanol at a 10-fold concentration and then passed through a syringe equipped with a 0.22 µm nylon membrane filter. Both parts were analyzed for malic acid quantification using HPLC-PAD (Figure S1). The %EE and %LC were calculated using Equations (5) and (6) [16]:

$$\%EE = \frac{(\text{Malic acid of precipitated})}{(\text{Malic acid of supernatant} + \text{Malic acid of precipitated})} \times 100 \quad (5)$$

$$\%LC = \frac{(\text{Malic acid of precipitated (mg)})}{(\text{Total lipids (mg)})} \times 100 \quad (6)$$

### 2.11. In Vitro Permeation Study

The artificial skin mimetic membrane (Strat-M<sup>®</sup> membrane, Merck KGaA, Darmstadt, Germany) is a pre-screening tool to evaluate skin permeation for cosmeceutical purposes and was used in this study as described by Opath et al. [17]. The membrane was soaked overnight with phosphate buffered saline (PBS), pH 7.4. The 10 mL of PBS pH 7.4 was filled into the receptor chamber of the FDC-6 Franz diffusion cell (Logan Instrument Corp., Somerset, NJ, USA). The membrane was positioned between the chamber and the donor. The 2 mL of the 2% ECE-loaded transethosomes and ECE solution (2% ECE in 20% ethanol) were loaded onto the donor and covered by foil and parafilm. The permeation condition was maintained at 37 ± 2 °C with the continuous stirrer at 600 rpm, according to the method of Opatha et al. [17] and Tawfeeka et al. [18]. The samples were withdrawn at 0.5, 1, 2, 4, 6, 8, 24, 32, and 48 h. The samples were measured for the amount of malic acid by HPLC-PAD. The cumulative amount permeated was constructed with time. The steady-state flux (J<sub>ss</sub>) was attained from the slope of the linear regression graph. The lag time was calculated from the extrapolation of the axis intercept. The permeability coefficient and enhancement ratio were calculated according to Equations (7) and (8):

$$P = J_{ss}/\text{initial concentration} \quad (7)$$

$$ER = J_{ss \text{ test}}/J_{ss \text{ control}} \quad (8)$$

### 2.12. Statistical Analysis

The results of our measurements were shown as mean values ± standard deviation, which were calculated as a result of three independent experiments. One-way ANOVA and Student's *t*-test were used for the analysis of the data to determine the extent of any differences between the results.

## 3. Results and Discussion

### 3.1. Extraction, Phytochemical Constituents, and Biological Activities of Ethanolic Extract of *C. carandas* L. (ECE)

A dry weight yield of 50.68% was obtained from the ethanolic extract of *C. carandas* L. (ECE). The study found that the extract of ECE contains four main active compounds related to skin brightening and anti-aging mechanisms, including malic acid, rutin, quercetin, and ursolic acid. The amounts of active ingredients were 44.18, 0.47, 0.03, and 0.002% (*w/w*) for malic acid, ursolic acid, rutin, and quercetin, respectively (Table S3). The procedure for determining ursolic acid, rutin, and quercetin was demonstrated in the Supplementary Materials. These compounds belong to the phenolic and flavonoid groups, which are known for their skin-brightening and anti-aging properties [19,20]. When comparing the amounts of these compounds, malic acid was found to be the most abundant in the ECE. It has a retention time (RT) of 8.898 min in comparison to the standard of malic acid (see

Figure 1). Academic reports indicate that malic acid, an AHA (alpha-hydroxy acid), has properties that help reduce wrinkles, even out skin tone, and diminish dark spots, such as post-inflammatory hyperpigmentation and melasma [21,22]. Therefore, this researcher chose malic acid as a key indicator of the quality of the ECE and its potential products in this study.

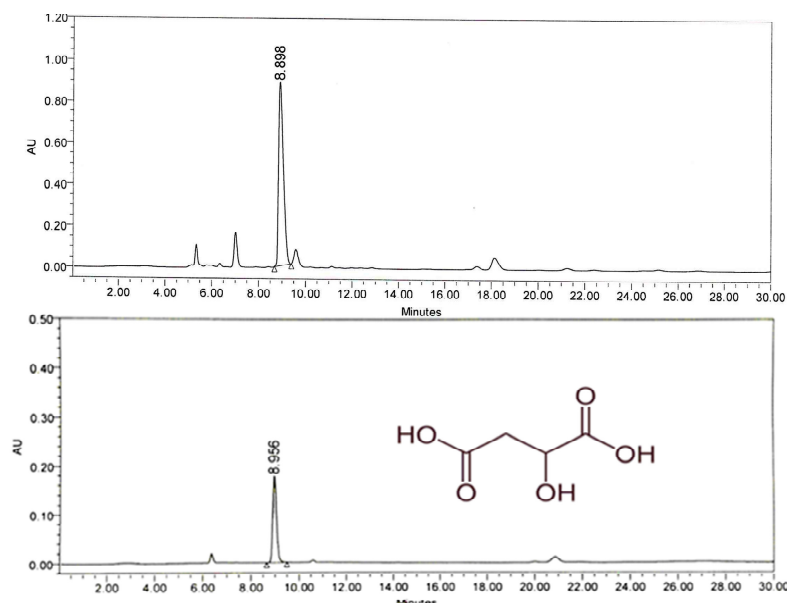


**Figure 1.** HPLC chromatogram of malic acid in ECE compared with the standard of malic acid.

A comparison of the anti-tyrosinase activity of ECE with kojic acid is presented in Table S4. The results indicated that the ECE had a dose-dependent anti-tyrosinase action, characterized by an  $IC_{50}$  value of 0.06 mg/mL, while kojic acid had an  $IC_{50}$  of 0.05 mg/mL.

Figure 2 depicts the cytotoxicity of ECE on normal human dermal fibroblast cells and melanoma cells ( $B_{16}F_{10}$ ). It was shown that the ECE showed low cytotoxicity towards normal human dermal fibroblasts and melanoma ( $B_{16}F_{10}$ ) cells. The viabilities were consistently higher than 80% for all tested dosages, ranging from 0.01 to 1.00 mg/mL. Using the cytotoxicity classification for natural ingredients, our extract might be classified as a potentially low-toxic ingredient. Cytotoxicity testing in melanoma cells ( $B_{16}F_{10}$ ) is performed before evaluating anti-tyrosinase activity to ensure that the compound does not cause excessive cell death or toxicity that would obscure the results of the subsequent analysis.

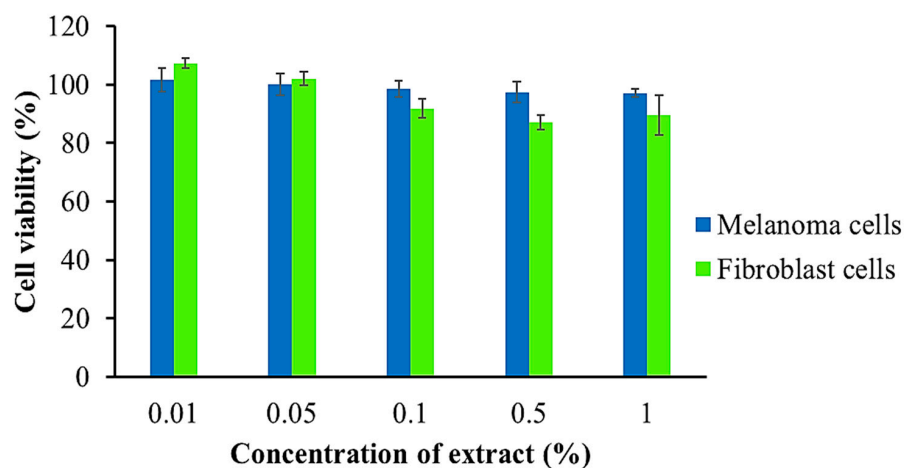


**Figure 2.** Cytotoxicity test of ECE on normal human dermal fibroblasts cells and melanoma ( $B_{16}F_{10}$ ) cells.

In addition, the ECE was tested for skin irritation using epidermal skin tissues in accordance with OECD Test No. 439: In vitro skin irritation: reconstructed human epidermis test methods. The test results were categorized into two groups: one group exhibiting no formation of purple formazan crystals, which suggests non-viable cells, and another group displaying dense formazan crystals, which provides evidence of viable cells. The cell viability rates are presented in Table 1. The positive control (PC), sodium dodecyl sulfate (SDS), has a skin tissue viability rate of  $0.78 \pm 0.07\%$ , whereas the negative control (NC), phosphate-buffered saline (PBS), provides a cell viability rate of  $99.99 \pm 6.41\%$ . The calculated cell viability rate for the ECE was  $92.38 \pm 3.96\%$ . The obtained result confirms that the ECE can be considered safe and appropriate for application in cosmetic or cosmeceutical products.

**Table 1.** Skin irritation test of ECE and ECE loaded in transethosomes on epidermal skin tissues using the OECD Test No. 439: In vitro skin irritation.





Samples	Simulated Skin Tissue After Testing and Incubation with MTT Solution	Cell Viability(%)	Results
Positive control		$0.78 \pm 0.07$	Irritant
Negative control		$99.99 \pm 6.41$	Non-irritant
2.00% ECE		$92.38 \pm 3.96$	Non-irritant
2.00% ECE loaded transethosomes		$103.59 \pm 3.70$	Non-irritant



Table 2 demonstrates that cellular tyrosinase inhibition, normal human dermal fibroblast proliferation, and collagen stimulation were investigated using doses of this extract ranging from 0.10 to 1.00 mg/mL.

**Table 2.** Effect of concentration of ECE on collagen stimulation and normal human dermal fibroblast proliferation.

Content of Extract (mg/mL)	Inhibition of Enzyme Tyrosinase in Melanoma Cells (%)	Collagen Stimulation (%)	Fibroblast Proliferation (%)
0.10	36.97 ± 7.63	24.31 ± 1.54	30.99 ± 6.75
0.50	49.85 ± 8.00	36.61 ± 2.48	35.70 ± 5.98
1.00	64.11 ± 6.97	60.09 ± 0.97	41.07 ± 4.21
Ascorbic acid (50 µg/mL)	-	17.81 ± 0.33	42.50 ± 5.48
Kojic acid (1.0 mg/mL)	81.96 ± 5.74	-	-
α-Arbutin (0.2 mg/mL)	38.02 ± 2.60	-	-

Melanoma cells (B<sub>16</sub>F<sub>10</sub>), which are produced from melanocytes (pigment-producing skin cells), express a high level of tyrosinase. Tyrosinase is a crucial enzyme in the biosynthesis of melanin, converting tyrosine to DOPA (dihydroxyphenylalanine) and finally to melanin. As a result, melanoma cells (B<sub>16</sub>F<sub>10</sub>) naturally have high tyrosinase activity. Furthermore, melanoma cells are specialized to manufacture melanin, making them an appropriate model for examining the enzyme activity of tyrosinase [23]. Therefore, a cellular enzyme tyrosinase inhibition experiment was employed to assess the efficacy of ECE as a whitening effect. The study revealed that the ability of ECE to inhibit the enzyme tyrosinase suggests their potential as an ingredient for skin lightening in cosmeceutical products. ECE exhibited dose-dependence of anti-tyrosinase activity in melanoma cells (B<sub>16</sub>F<sub>10</sub>), with inhibition values ranging from 36.97 to 64.11% as the extract concentration was increased from 0.10 to 1.00 mg/mL (Table 2). Vitamin C, phenolic compounds, flavonoids, and malic acid are the primary components responsible for the anti-tyrosinase activity of fruit extract. The outcome exhibited identical characteristics to those reported by Khunchalee and Charoenboon [23]. The observation that the ECE exhibited the highest tyrosinase inhibition at 77.65% may be attributed to the high content of flavonoids, vitamin C, and anthocyanin in the ECE. These flavonoids and anthocyanins possess the capacity to inhibit both tyrosinase and melanogenesis.

Increasing amounts of ECE from 0.10 to 1.00 mg/mL resulted in normal human dermal fibroblast proliferation values ranging from 30.99 ± 6.75 to 41.07 ± 4.21%, indicating a dose-dependent effect (Table 2). The data shown in Table 2 demonstrates a positive correlation between an increase in normal human dermal fibroblast proliferation and the stimulation of collagen synthesis. A comparative ELISA assay was used to assess the collagen synthesis-stimulating capacity of ECE compared to the positive control ascorbic acid. Results indicated that the collagen production-boosting effect of this extract increased significantly ( $p < 0.05$ ) from 24.31 ± 1.54 to 60.09 ± 0.97% as the concentration of the extract was increased from 0.10 to 1.00 mg/mL (Table 2). The result should be attributed to the composition of ECE, which includes phenolics, flavonoids, vitamin C, and malic acid. These components enable the extract to enhance the growth of fibroblasts and stimulate the creation of collagen. Fundamentally, the process of skin aging has been correlated to a reduction in the content of collagen in the skin, resulting in obvious indications, such as wrinkles and elasticity. One of the contributing factors to collagen deficiency is a decrease in synthesis. At present, there is a growing interest in compounds that are capable of promoting collagen synthesis for their potential use in skin anti-aging cosmetic formulations. Consequently, the ECE possesses strong anti-aging and skin-whitening properties, which makes it quite a promising new cosmeceutical agent.

### 3.2. Optimization of ECE Loaded in Transethosome Formulations

The optimal conditions for the formation of transethosomes loaded with ECE were evaluated by comparing the different techniques in Equations (1)–(3) (Table 3). Equation (3), using a probe sonicator for 5 min, produced the smallest particle size ( $463.77 \pm 31.22$  nm) and the highest negative zeta potential ( $-31.37 \pm 0.42$  mV). Formulations 1 and 2 were larger sizes, exceeding 500 nm, making it difficult for active substances to permeate from the outside to the deeper skin [24,25]. Hence, Formulation 3 was chosen for further development. Despite its relatively high polydispersity index of  $0.64 \pm 0.02$ ; therefore, it was refined by experimentally investigating several edge activators in Formulation 3–5. The result revealed that Formulation 3, including Tween 80, still generated the smallest size due to the long carbon chain ( $C_{18}$ ) of polysorbate 80. Carbon chains of greater length result in smaller sizes compared to surfactants with shorter carbon chains, such as  $C_{12}$  [26]. Moreover, the HLB value of polysorbate 80 is comparatively lower than that of the other two surfactants. An elevated HLB value enhances hydrophilicity, resulting in increased surface free energy, and hence larger sizes were obtained [26]. These findings correlate with prior research indicating that polysorbate 80 produces smaller particle sizes in comparison to PEG 40 hydrogenated castor oil and polysorbate 20 [27,28]. In order to achieve a smaller size ( $379.60 \pm 85.94$  nm), which is consistent with previous results [29], and a more uniform particle size distribution ( $0.54 \pm 0.03$ ), further development was carried out by reducing the ethanol concentration to 20.0% (*v/v*) in Formulation 6. Nevertheless, it was seen that the zeta potential decreased to  $-22.80 \pm 1.73$  mV, which corresponds to prior research that found a positive correlation between higher ethanol concentration and more negative charges on the particles [30]. Further studies were conducted by changing the initial solvent from absolute ethanol to 70.0% (*v/v*) ethanol in Formulation 7, which resulted in a slight increase in size, but provided particle size distribution values that were more consistent, with a zeta potential still remaining below  $-30$  mV. This is because the ECE used was extracted with 70.0% (*v/v*) ethanol, resulting in better solubility and improved binding capabilities with the particles, resulting in a decrease in size distribution and a larger size were obtained. In previous studies, the formulation used absolute ethanol to dissolve the ECE; hence, this may have resulted in incomplete solubility of the extract, causing the presence of extract crystals dispersed in the system, leading to more extensive particle size distribution, which may affect the zeta potential. This ratio was then further developed by adjusting the sonicator power in Formulation 8–10. It was found that Formulation 10, using 10.0% power, yielded the smallest size ( $277.47 \pm 21.36$  nm) and had a particle size distribution value of less than 0.50, indicating a uniform particle size distribution. However, the zeta potential obtained was  $-24.80 \pm 0.87$  mV. Since formulation 10 produced the smallest size and a uniform particle size distribution, this condition was selected for further study in preparing transethosomes with different concentrations of extract to enhance stability and deep skin penetration.

**Table 3.** Size, polydisperse index (PDI), and zeta potential of transethosomes in different formulations.

Formula	Physicochemical Properties		
	Size (nm)	Polydisperse Index (PDI)	Zeta Potential (mV)
1	$834.43 \pm 138.92$	$0.47 \pm 0.12$	$-22.20 \pm 0.78$
2	$504.00 \pm 42.96$	$0.47 \pm 0.01$	$-24.13 \pm 0.32$
3	$463.77 \pm 31.22$	$0.64 \pm 0.02$	$-31.37 \pm 0.42$
4	$649.67 \pm 52.64$	$0.35 \pm 0.01$	$-24.00 \pm 0.87$
5	$345.17 \pm 122.17$	$1.00 \pm 0.00$	$-26.07 \pm 0.83$
6	$379.60 \pm 85.94$	$0.54 \pm 0.03$	$-22.80 \pm 1.73$
7	$412.43 \pm 46.52$	$0.57 \pm 0.01$	$-30.30 \pm 0.10$

Table 3. Cont.

Formula	Physicochemical Properties		
	Size (nm)	Polydisperse Index (PDI)	Zeta Potential (mV)
8	399.23 ± 61.01	0.72 ± 0.09	−20.37 ± 1.27
9	232.40 ± 77.08	0.61 ± 0.11	−19.80 ± 1.87
10	277.47 ± 21.36	0.45 ± 0.00	−24.80 ± 0.87

### 3.3. Effect of Concentration of ECE Loaded in Transethosomes: Formulation and Characterization

The development of transethosomes was optimized by varying the most appropriate conditions. The optimal transethosomes formula was determined to be 1.00% (*w/v*) phosphatidylcholine, 28.55% (*v/v*) ethanol, and 0.10% (*w/w*) polysorbate 80. In this study, the transferosome system was used to encapsulate extracts of ECE at concentrations of 0.50%, 1.00%, and 2.00% (*w/w*). As depicted in Figure 3, the transethosomes without the extract exhibited transparency with a light yellow color. The transethosomes displayed a pink-red color as a result of the inclusion of ECE extracts. After that, the physical properties of the transethosomes were investigated, including their size, zeta potential, size distribution, and the percentage of encapsulation efficacy of malic acid in ECE. The study of the optimal conditions for the production of transethosomes revealed that the most appropriate formulation for transethosomes comprises 1.00% phosphatidylcholine (*w/v*), 28.55% ethanol, and 0.10% polysorbate 80. This formulation results in particles with a size of  $83.36 \pm 12.06$  nm, a size distribution (PDI) of  $0.25 \pm 0.01$ , and a zeta potential of  $-33.77 \pm 0.71$  mV. Furthermore, the effect of the concentration of ECE on the characteristics of the transethosomes, such as particle size, size distribution, and zeta potential, was investigated and presented in Table 4.

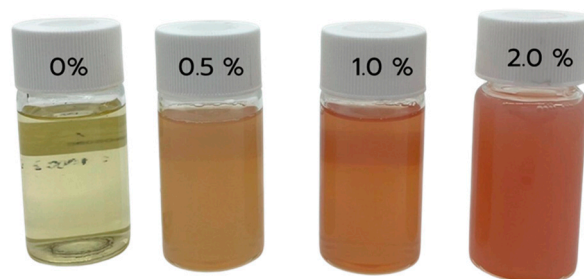


Figure 3. Appearance of various concentrations of ECE-loaded transethosomes.

The study revealed that the formulation containing 2.00% ECE exhibited a particle size of  $277.47 \pm 21.36$  nm and a size distribution of  $0.45 \pm 0.00$  (Table 4). These values were significantly greater ( $p < 0.05$ ) than those of the formulations containing 1.00% and 0.50% ECE. Moreover, the zeta potential of the 2.00% ECE-loaded transethosomes was measured to be  $-24.80 \pm 0.87$  mV, indicating a reduced negative value in comparison to the 1.00% ( $-31.43 \pm 1.53$  mV) and 0.50% ( $-30.43 \pm 0.42$  mV) ECE-loaded transethosomes. No statistically significant difference ( $p < 0.05$ ) was seen between the formulations containing 0.50% and 1.00% ECE in all parameters. The increase in particle size of the transethosomes with 2.00% ECE was attributed to the aggregation of the head groups at the particle surface, as well as the enhanced encapsulation of the active compounds, resulting in the expansion of the transferosome walls. This observation corresponds to previous studies that have demonstrated a positive correlation between increased concentrations of extract and larger particle size [31,32]. Furthermore, transethosomes containing 0.50% and 1.00% ECE had zeta potentials less than  $-30$  mV, showing significant particle repulsion that contributes to stability and prevents precipitation [33]. In contrast, increasing the ECE concentration to 2.00% resulted in a reduced negative zeta potential, which has previously been shown to decrease with larger extract quantities [32,34]. All formulations exhibited a size distribution

of less than 0.5, indicating comparable size distributions [35]. Based on these findings, the transethosomes formulation containing 2.00% ECE was chosen for further investigation into skin penetration and safety, with the goal of developing it as a cosmeceutical agent for skin brightening and anti-aging.

**Table 4.** Effect of ECE content on size, polydisperse index (PDI), zeta potential, encapsulation efficiency, and loading capacity of transethosomes.

Content of ECE (%)	Size (nm)	Polydisperse Index (PDI)	Zeta Potential (mV)	Encapsulation Efficacy (%)	Loading Capacity (%)
0.50	213.57 ± 13.54 <sup>a</sup>	0.34 ± 0.04 <sup>a</sup>	−30.43 ± 0.42 <sup>a</sup>	49.81 ± 2.07 <sup>a</sup>	2.71 ± 0.35 <sup>a</sup>
1.00	202.87 ± 5.22 <sup>a</sup>	0.36 ± 0.05 <sup>a</sup>	−31.43 ± 1.53 <sup>a</sup>	67.77 ± 5.52 <sup>a</sup>	7.18 ± 0.88 <sup>b</sup>
2.00	277.47 ± 21.36 <sup>b</sup>	0.45 ± 0.00 <sup>b</sup>	−24.80 ± 0.87 <sup>b</sup>	63.02 ± 15.35 <sup>a</sup>	14.70 ± 1.31 <sup>c</sup>

<sup>abc</sup> indicated statistically significant ( $p < 0.05$ ) between groups.

The study on the % encapsulation of malic acid in transethosomes (Table 4) found that there were no statistically significant differences between the formulations ( $p < 0.05$ ). However, the percentage of encapsulation increased slightly with higher concentrations of the ECE, which is consistent with previous studies that showed increased percentages of encapsulation with higher concentrations of active ingredients [34]. The percentage of loading capacity demonstrates that an increased ECE concentration leads to an improved ECE active ingredient loading capacity. All formulations exhibited a limited loading capacity of the active ingredient in ECE due to the migration and loss of the ECE active ingredient in the external aqueous phase [36].

The morphology of blank transethosomes and 2.00% ECE-loaded transethosomes (Figure 4) illustrates that both particles were spherical shapes.

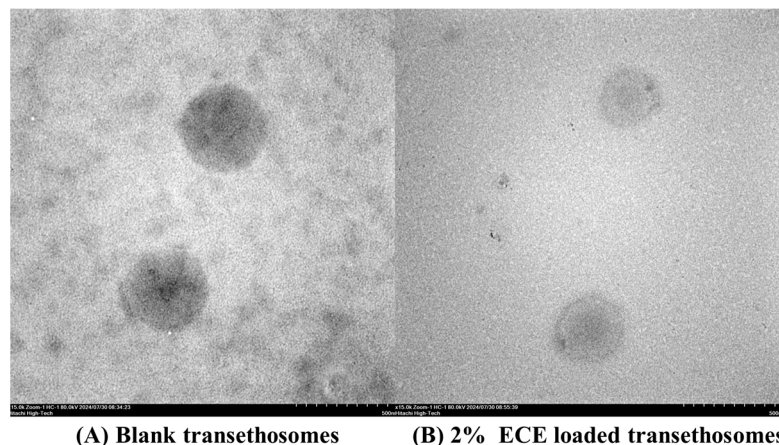


**Figure 4.** Morphology of transethosomes by TEM, blank transethosomes (A), and 2.00% ECE-loaded transethosomes (B).

The *in vitro* permeation study exhibited that 2.00% ECE-loaded transethosomes had a higher profile cumulative amount permeated of malic acid and enhancement ratio than 2.00% ethanolic extract solution (Figure 5).

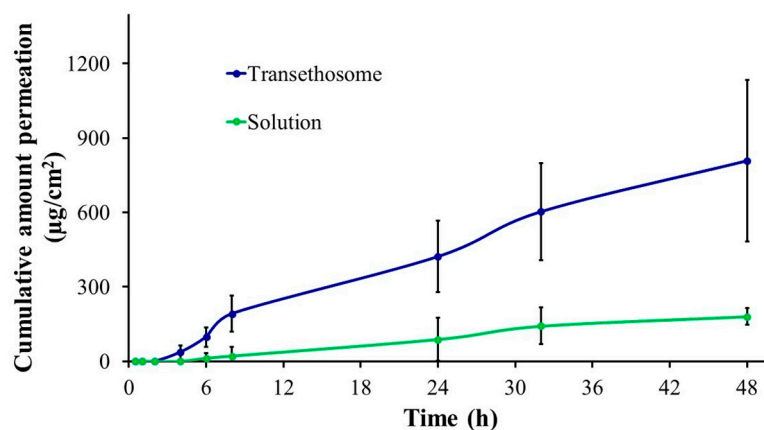


**Figure 5.** In vitro skin permeation of 2.00% ECE-loaded transethosomes compared with 2.00% ECE solution.

Furthermore, ECE-loaded transethosomes demonstrated significantly increased flux ( $17.27 \pm 6.68 \mu\text{g}/\text{cm}^2/\text{h}$ ), Q48 permeated ( $808.78 \pm 324.64 \mu\text{g}/\text{cm}^2$ ), and permeability coefficient ( $11.31 \pm 4.37 \text{ cm}/\text{h}$ ) more than ethanolic extract solution (Table 5). Nonetheless, ECE-loaded transethosomes exhibited a slightly lower lag time ( $0.51 \pm 5.81 \text{ h}$ ) than the solution ( $2.28 \pm 4.75 \text{ h}$ ), indicating that the ECE in the transethosome form shortens the initial permeation time compared to the ECE solution form (Table 5). The highest permeability of transethosomes was attributed to vesicle deformability and lipid perturbation across the membrane [37,38]. Additionally, ethanol, a component of transethosomes, provides high flexibility and increased lipid fluidity of membranes [39], while polysorbate 80 acts as an edge activator, contributing to high flexibility and deformability [40]. Furthermore, the small particle size of transethosomes and the enhanced solubility of the extract with transethosomes increase skin permeation [40]. In this study, in vitro skin permeation using Strat-M<sup>®</sup> Membrane (Merck KGaA, Darmstadt, Germany) is employed as a pre-screening tool to predict transethosome permeation efficacy. In future investigations, we will focus on ex vivo skin permeation using porcine skin and measure the retention of the active component. This will be followed by confocal microscopy to measure the depth of skin penetration.

**Table 5.** In vitro skin permeation steady-state flux, lag time, enhancement ratio (ER), permeability coefficient, and cumulative amount of 2.00% ECE-loaded transethosomes compared with 2.00% ECE solution.

Formulation	Flux ( $\mu\text{g}/\text{cm}^2/\text{h}$ )	Lag Time (h)	ER	$P \times 10^{-3}$ (cm/h)	Q 48 h ( $\mu\text{g}/\text{cm}^2$ )
2.00% ECE-loaded transethosomes	$17.27 \pm 6.68^*$	$0.51 \pm 5.81$	4.14	$11.31 \pm 4.37^*$	$808.78 \pm 324.64^*$
2.00% ECE solution	$4.18 \pm 1.55^*$	$2.28 \pm 4.75$	1.00	$3.92 \pm 1.46^*$	$180.84 \pm 33.59^*$

ER: enhancement ratio, P: permeability coefficient, Q: cumulative amount. \* Indicated statically significant ( $p < 0.05$ ) between groups.

The investigation revealed that the formulation of 1.00 and 2.00% ECE loaded in transethosomes exhibited low cytotoxicity towards normal human dermal fibroblast cells within the concentration range of 1.00–10.00 mg/mL (Figure 6). Cell viability over 80.0% was reported at all assessed concentrations. The findings indicate that the incorporation of ECE into transethosomes at concentrations ranging from 1.00 to 10.00 mg/mL has potential for use in the formulation of cosmeceutical products.

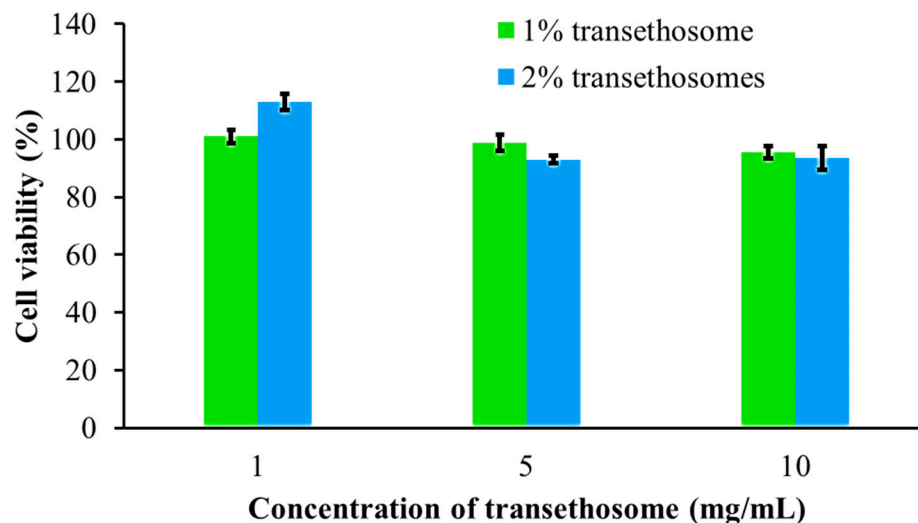


**Figure 6.** Cytotoxicity test of 1.00 and 2.00% ECE-loaded transethosomes on normal human dermal fibroblast cells.

The skin irritation of ECE loaded in transethosomes was evaluated on epidermal skin tissues using OECD Test No. 439: In vitro skin irritation: reconstructed human epidermis test methods, as illustrated in Figure 7 and Table 1. The test results were classified into two categories: one group showing no production of purple formazan crystals, indicating non-viable cells, and another group exhibiting dense formazan crystals, indicating live cells. Table 1 displays the cell viability rates. The positive control (PC), sodium dodecyl sulfate (SDS), exhibits a skin tissue viability rate of  $0.78 \pm 0.07\%$ , whereas the negative control (NC), phosphate-buffered saline (PBS), demonstrates a cell viability rate of  $99.99 \pm 6.41\%$ . The determined cell viability rate for the ECE loaded in transethosomes was  $103.59 \pm 3.70\%$ . The results indicate that the ECE loaded in transethosome formulation is safe and suitable for use in cosmetic or cosmeceutical products, hence enabling improvements in skin brightness and anti-aging effects.

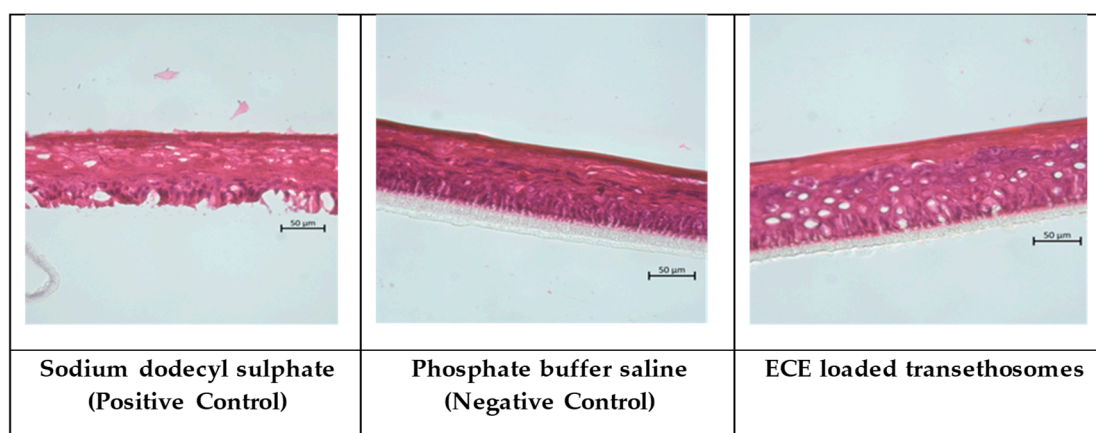


**Figure 7.** Cross-sectional image of skin tissue under an inverted microscope ( $40\times$  magnification).

#### 4. Conclusions

In this study, *Carissa carandas* L. was extracted using ultrasonic assisted extraction (UEA) with a water-ethanol solvent mixture. *C. carandas* L. extract (ECE) inhibited the enzyme tyrosinase, increased the proliferation of normal human dermal fibroblasts, and stimulated the formation of collagen type I, demonstrating its efficacy as an anti-aging and skin whitening agent. Transethosomes were subsequently developed to encapsulate ECE for applications on the skin. Transethosomes were also successfully generated using the

sonication technique with an appropriate formulation of 1.00% (*w/v*) phosphatidylcholine, 0.10% (*w/v*) polysorbate 80, and 28.55% (*v/v*) ethanol. The percentages of ECE encapsulated in transethosomes increased slightly as the extract concentrations increased. When compared to the liquid extract, ECE loaded in transethosomes improved skin penetration. Furthermore, transethosomes containing ECE demonstrated low cytotoxicity in normal human dermal fibroblast cells and caused no skin irritation when tested on reconstructed human epidermal skin. Therefore, ECE-loaded transethosomes are highly potent anti-aging and skin-whitening agents, making them a promising novel cosmeceutical ingredient. This research has the potential to develop a local fruit into a globally recognized active ingredient for use in health and cosmeceutical products.

**Supplementary Materials:** The following supporting information can be downloaded at: <https://www.mdpi.com/article/10.3390/cosmetics11060199/s1>, Table S1: Composition and condition of ECE-loaded transethosome preparations; Table S2: Effect of concentrations of ECE loaded in transethosomes; Table S3: Amount of active ingredients of ECE; Table S4: Anti-tyrosinase activity assay of ECE.; Figure S1: Example HPLC chromatogram of malic acid in ECE (*Carissa carandas* L.) extract in the precipitate (a) and supernatant (b) of transethosomes.

**Author Contributions:** Conceptualization, S.S. and W.T.; methodology, S.S., S.R., T.M. and P.K.; software, S.S., P.P. and K.O.; validation, S.S. and T.M.; formal analysis, S.S. and P.P.; investigation, S.S., S.I. and T.M.; resources, S.S. and T.M.; data curation, S.S.; writing—original draft preparation, S.S. and P.P.; writing—review and editing, S.S., S.I. and T.M.; visualization, P.P. and S.S.; supervision, S.S. and T.M.; project administration, S.S.; funding acquisition, S.S. All authors have read and agreed to the published version of the manuscript.

**Funding:** This research received funding from the Thailand Institute of Scientific and Technological Research, Ministry of Higher Education, Science, Research, and Innovation, Thailand; grant number [6718101064].

**Institutional Review Board Statement:** Not applicable.

**Informed Consent Statement:** Not applicable.

**Data Availability Statement:** All raw data are included in supporting information or from the authors.

**Acknowledgments:** The authors are grateful to the Thailand Institute of Scientific and Technological Research, Ministry of Higher Education, Science, Research, and Innovation, for funding the scholarship to perform this research. The assistance of staff at the Expert Centre of Innovative Herbal Products, Thailand Institute of Scientific and Technological Research with Zeta Sizer Nano ZS, High Performance Liquid Chromatography, TEM, and cell experiments is also acknowledged.

**Conflicts of Interest:** The authors declare that they have no known competing financial interest or personal relationships that could have appeared to influence the work reported in this paper.

## References

1. Nadechanok, J.; Charinrat, S.; Nattawut, L.; Arpa, P. The Evaluation of Antioxidant and Antityrosinase Efficacy of *Carissa carandas* Fruit Extracts and the Development of a Preliminary Skincare Product. *J. Appl. Pharm. Sci.* **2020**, *11*, 153–157. [[CrossRef](#)]
2. Khuaneekaphan, M.; Khobjai, W.; Noysang, C.; Wisidsri, N.; Thungmungmee, S. Bioactivities of Karanda (*Carissa carandas* Linn.) Fruit Extracts for Novel Cosmeceutical Applications. *J. Adv. Pharm. Technol. Res.* **2021**, *12*, 162. [[CrossRef](#)] [[PubMed](#)]
3. Singh, S.; Bajpai, M.; Mishra, P. *Carissa carandas* L.—Phyto-Pharmacological Review. *J. Pharm. Pharmacol.* **2020**, *72*, 1694–1714. [[CrossRef](#)] [[PubMed](#)]
4. Mishra, C.K.; Pattnaik, A.K.; Dagur, P.; Kumar, D.; Ghosh, M. Excision and Incision Wound Healing Activity of Apigenin (4',5,7-Trihydroxyflavone) Containing Extracts of *Carissa carandas* Linn. Fruits. *Pharmacogn. Mag.* **2022**, *18*, 502–509. [[CrossRef](#)]
5. Toobpeng, N.; Powthong, P.; Suntornthiticharoen, P. Evaluation of Antioxidant and Antibacterial Activities of Fresh and Freeze-dried Selected Fruit Juices. *Asian J. Pharm. Clin. Res.* **2017**, *10*, 156–160. [[CrossRef](#)]
6. Saher, S.; Narnawre, S.; Patil, J. Evaluation of Phytochemical and Pharmacological Activity of *Carissa carandas* L. Fruits at Three Different Stages of Maturation. *Drug Res. (Stuttg)* **2020**, *70*, 80–85. [[CrossRef](#)]
7. Neimkhum, W.; Anuchapreeda, S.; Lin, W.-C.; Lue, S.-C.; Lee, K.-H.; Chaiyana, W. Effects of *Carissa carandas* Linn. Fruit, Pulp, Leaf, and Seed on Oxidation, Inflammation, Tyrosinase, Matrix Metalloproteinase, Elastase, and Hyaluronidase Inhibition. *Antioxidants* **2021**, *10*, 1345. [[CrossRef](#)]

8. Bhokare, S.G.; Dongaonkar, C.C.; Lahane, S.V.; Sawale, V.S.; Thombare, M.S. Herbal Novel Drug Delivery—A Review. *World J. Pharm. Pharm. Sci.* **2016**, *5*, 593–611.
9. Manosroi, A.; Khanrin, P.; Lohcharoenkal, W.; Werner, R.G.; Götz, F.; Manosroi, W.; Manosroi, J. Transdermal Absorption Enhancement through Rat Skin of Gallidermin Loaded in Niosomes. *Int. J. Pharm.* **2010**, *392*, 304–310. [[CrossRef](#)]
10. Casanova, F.; Santos, L. Encapsulation of Cosmetic Active Ingredients for Topical Application—A Review. *J. Microencapsul.* **2016**, *33*, 1–17. [[CrossRef](#)]
11. Raj, A.; Dua, K.; Nair, R.S.; Sarath Chandran, C.; Alex, A.T. Transethosome: An Ultra-Deformable Ethanolic Vesicle for Enhanced Transdermal Drug Delivery. *Chem. Phys. Lipids* **2023**, *255*, 105315. [[CrossRef](#)] [[PubMed](#)]
12. Ferrara, F.; Benedusi, M.; Sguizzato, M.; Cortesi, R.; Baldisserotto, A.; Buzzi, R.; Valacchi, G.; Esposito, E. Ethosomes and Transethosomes as Cutaneous Delivery Systems for Quercetin: A Preliminary Study on Melanoma Cells. *Pharmaceutics* **2022**, *14*, 1038. [[CrossRef](#)] [[PubMed](#)]
13. Sguizzato, M.; Ferrara, F.; Hallan, S.S.; Baldisserotto, A.; Drechsler, M.; Malatesta, M.; Costanzo, M.; Cortesi, R.; Puglia, C.; Valacchi, G.; et al. Ethosomes and Transethosomes for Mangiferin Transdermal Delivery. *Antioxidants* **2021**, *10*, 768. [[CrossRef](#)] [[PubMed](#)]
14. Manosroi, A.; Boonpisuttinant, K.; Winitchai, S.; Manosroi, W.; Manosroi, J. Free Radical Scavenging and Tyrosinase Inhibition Activity of Oils and Sericin Extracted from Thai Native Silkworms (*Bombyx mori*). *Pharm. Biol.* **2010**, *48*, 855–860. [[CrossRef](#)] [[PubMed](#)]
15. Manosroi, A.; Saraphanchotiwitthaya, A.; Manosroi, J. In Vivo Immunomodulating Activity of Wood Extracts from *Clausena excavata* Burm. f. *J. Ethnopharmacol.* **2005**, *102*, 5–9. [[CrossRef](#)]
16. Bollareddy, S.R.; Krishna, V.; Roy, G.; Dasari, D.; Dhar, A.; Venuganti, V.V.K. Transfersome Hydrogel Containing 5-Fluorouracil and Etodolac Combination for Synergistic Oral Cancer Treatment. *AAPS Pharm. Sci. Tech.* **2022**, *23*, 70. [[CrossRef](#)]
17. Opatha, S.A.T.; Titapiwatanakun, V.; Boonpisutiinant, K.; Chutoprapat, R. Preparation, Characterization and Permeation Study of Topical Gel Loaded with Transfersomes Containing Asiatic Acid. *Molecules* **2022**, *27*, 4865. [[CrossRef](#)]
18. Tawfeek, H.M.; Abdellatif, A.A.H.; Abdel-Aleem, J.A.; Hassan, Y.A.; Fathalla, D. Transfersomal Gel Nanocarriers for Enhancement the Permeation of Lornoxicam. *J. Drug Deliv. Sci. Technol.* **2020**, *56*, 101540. [[CrossRef](#)]
19. de Lima Cherubim, D.J.; Buzanello Martins, C.V.; Oliveira Fariña, L.; da Silva de Lucca, R.A. Polyphenols as Natural Antioxidants in Cosmetics Applications. *J. Cosmet. Dermatol.* **2020**, *19*, 33–37. [[CrossRef](#)]
20. Przybylska-Balcererek, A.; Stuper-Szablewska, K. Phenolic Acids Used in the Cosmetics Industry as Natural Antioxidants. *EJMT* **2019**, *4*, 24–32.
21. Krstonošić, V.; Ćirin, D. Are Cosmetics Based on Alpha Hydroxy Acids Safe to Use When Purchased over the Internet? *Toxicol. Ind. Health* **2022**, *38*, 835–838. [[CrossRef](#)]
22. Tang, S.-C.; Yang, J.-H. Dual Effects of Alpha-Hydroxy Acids on the Skin. *Molecules* **2018**, *23*, 863. [[CrossRef](#)] [[PubMed](#)]
23. Khunchalee, J.; Charoenboon, P. The Study of Free Radical Scavenging, Total Phenolic Contents and Tyrosinase Inhibition Activity of Crude Extract from *Carissa carandas* Linn. *Creat. Sci.* **2019**, *11*, 26–34.
24. Friedman, N.; Dagan, A.; Elia, J.; Merims, S.; Benny, O. Physical Properties of Gold Nanoparticles Affect Skin Penetration via Hair Follicles. *Nanomed. Nanotechnol. Biol. Med.* **2021**, *36*, 102414. [[CrossRef](#)]
25. Su, R.; Fan, W.; Yu, Q.; Dong, X.; Qi, J.; Zhu, Q.; Zhao, W.; Wu, W.; Chen, Z.; Li, Y.; et al. Size-Dependent Penetration of Nanoemulsions into Epidermis and Hair Follicles: Implications for Transdermal Delivery and Immunization. *Oncotarget* **2017**, *8*, 38214–38226. [[CrossRef](#)]
26. Bnyan, R.; Khan, I.; Ehtezazi, T.; Saleem, I.; Gordon, S.; O'Neill, F.; Roberts, M. Surfactant Effects on Lipid-Based Vesicles Properties. *J. Pharm. Sci.* **2018**, *107*, 1237–1246. [[CrossRef](#)] [[PubMed](#)]
27. Nagaraju, P.G.; Sengupta, P.; Chicgovinda, P.P.; Rao, P.J. Nanoencapsulation of Clove Oil and Study of Physicochemical Properties, Cytotoxic, Hemolytic, and Antioxidant Activities. *J. Food Process. Eng.* **2021**, *44*, e13645. [[CrossRef](#)]
28. Salem, H.F.; Kharshoum, R.M.; Abou-Taleb, H.A.; Farouk, H.O.; Zaki, R.M. Fabrication and Appraisal of Simvastatin via Tailored Niosomal Nanovesicles for Transdermal Delivery Enhancement: In Vitro and In Vivo Assessment. *Pharmaceutics* **2021**, *13*, 138. [[CrossRef](#)]
29. Chiu, C.-W.; Chang, C.-H.; Yang, Y.-M. Ethanol Effects on the Gelation Behavior of  $\alpha$ -Tocopherol Acetate-Encapsulated Ethosomes with Water-Soluble Polymers. *Colloid. Polym. Sci.* **2013**, *291*, 1341–1352. [[CrossRef](#)]
30. Qureshi, M.I.; Jamil, Q.A.; Usman, F.; Wani, T.A.; Farooq, M.; Shah, H.S.; Ahmad, H.; Khalil, R.; Sajjad, M.; Zargar, S.; et al. Tioconazole-Loaded Transethosomal Gel Using Box–Behnken Design for Topical Applications: In Vitro, In Vivo, and Molecular Docking Approaches. *Gels* **2023**, *9*, 767. [[CrossRef](#)]
31. Dudhipala, N.; Phasha Mohammed, R.; Adel Ali Youssef, A.; Banala, N. Effect of Lipid and Edge Activator Concentration on Development of Aceclofenac-Loaded Transfersomes Gel for Transdermal Application: In Vitro and Ex Vivo Skin Permeation. *Drug Dev. Ind. Pharm.* **2020**, *46*, 1334–1344. [[CrossRef](#)] [[PubMed](#)]
32. Avadhani, K.S.; Manikkath, J.; Tiwari, M.; Chandrasekhar, M.; Godavarthi, A.; Vidya, S.M.; Hariharapura, R.C.; Kalthur, G.; Udupa, N.; Mutalik, S. Skin Delivery of Epigallocatechin-3-Gallate (EGCG) and Hyaluronic Acid Loaded Nano-Transfersomes for Antioxidant and Anti-Aging Effects in UV Radiation Induced Skin Damage. *Drug Deliv.* **2017**, *24*, 61–74. [[CrossRef](#)] [[PubMed](#)]



33. Ferreira, M.A.; De Almeida Júnior, R.F.; Onofre, T.S.; Casadei, B.R.; Farias, K.J.S.; Severino, P.; De Oliveira Franco, C.F.; Raffin, F.N.; De Lima E Moura, T.F.A.; De Melo Barbosa, R. Annatto Oil Loaded Nanostructured Lipid Carriers: A Potential New Treatment for Cutaneous Leishmaniasis. *Pharmaceutics* **2021**, *13*, 1912. [[CrossRef](#)] [[PubMed](#)]
34. Yeo, S.; Yoon, I.; Lee, W.K. Design and Characterisation of pH-Responsive Photosensitiser-Loaded Nano-Transfersomes for Enhanced Photodynamic Therapy. *Pharmaceutics* **2022**, *14*, 210. [[CrossRef](#)] [[PubMed](#)]
35. Naguib, M.J.; Salah, S.; Abdel Halim, S.A.; Badr-Eldin, S.M. Investigating the Potential of Utilizing Glycosomes as a Novel Vesicular Platform for Enhancing Intranasal Delivery of Lacidipine. *Int. J. Pharm.* **2020**, *582*, 119302. [[CrossRef](#)]
36. Cui, F.; Shi, K.; Zhang, L.; Tao, A.; Kawashima, Y. Biodegradable Nanoparticles Loaded with Insulin–Phospholipid Complex for Oral Delivery: Preparation, in Vitro Characterization and In Vivo Evaluation. *J. Control. Release* **2006**, *114*, 242–250. [[CrossRef](#)]
37. Hassan, A.S.; Hofni, A.; Abourehab, M.A.; Abdel-Rahman, I.A. Ginger Extract–Loaded Transethosomes for Effective Transdermal Permeation and Anti-Inflammation in Rat Model. *Int. J. Nanomed.* **2023**, *18*, 1259–1280. [[CrossRef](#)]
38. Munir, M.; Zaman, M.; Waqar, M.A.; Hameed, H.; Riaz, T. A Comprehensive Review on Transethosomes as a Novel Vesicular Approach for Drug Delivery through Transdermal Route. *J. Liposome Res.* **2024**, *34*, 203–218. [[CrossRef](#)]
39. Albash, R.; Abdelbary, A.; Refai, H.; El-Nabarawi, M. Use of Transethosomes for Enhancing the Transdermal Delivery of Olmesartan Medoxomil: In Vitro, Ex Vivo, and in Vivo Evaluation. *Int. J. Nanomed.* **2019**, *14*, 1953–1968. [[CrossRef](#)]
40. Patil, S.; Dandagi, P.M.; Kazi, T.; Hulyalkar, S.; Biradar, P.; Kumbar, V. A DoE-Based Development and Characterization of Nadifloxacin-Loaded Transethosomal Gel for the Treatment of Acne Vulgaris. *Futur. J. Pharm. Sci.* **2024**, *10*, 46. [[CrossRef](#)]

**Disclaimer/Publisher’s Note:** The statements, opinions and data contained in all publications are solely those of the individual author(s) and contributor(s) and not of MDPI and/or the editor(s). MDPI and/or the editor(s) disclaim responsibility for any injury to people or property resulting from any ideas, methods, instructions or products referred to in the content.